

## **Journal of Electronic & Information Systems**

https://journals.bilpubgroup.com/index.php/jeis

### **ARTICLE**

# Precise Spacecraft Attitude and Angular Velocity Estimates Using Cubature Kalman Filter on Intensely Distorted One-Axis Magnetometer Measurements

Tamer Mekky Ahmed Habib 1,2 10

#### **ABSTRACT**

Magnetometers are widely used spacecraft attitude sensors due to their numerous advantages. Typically, fully observing a spacecraft's attitude requires the use of at least two distinct sensor types. Thus, relying exclusively on a magnetometer introduces major challenges for estimation algorithms. The problem of spacecraft attitude estimation based on magnetometer measurements is generally nonlinear. Cubature Kalman Filter (CKF) is considered as a newly developed filter that addresses the problem of state estimation for nonlinear systems. The current research article develops a CKF algorithm that utilizes magnetometer measurements as a sole spacecraft attitude sensor. The developed algorithm provides multiple benefits over traditional methods, offering exceptional accuracy comparable to other Extended Kalman Filter based (EKF-based) algorithms. The developed CKF has a resistance to significant initial estimation errors. The proposed CKF algorithm functions in every spacecraft operational mode, consistently delivering precise results. Even when measurements are severely noisy, CKF achieves an accuracy of better than 0.24 degree  $(1-\sigma)$  approximately in each axis. This accuracy enabled the magnetometer to serve as the sole source of spacecraft attitude information despite having one or two faulty channels out of three. A benchmarking for the proposed CKF is given against many other intensely verified EKF-based algorithms to present a quantitative comparison. This comparison could help the designer of the spacecraft Attitude and

#### \*CORRESPONDING AUTHOR:

Tamer Mekky Ahmed Habib, Spacecraft Dynamics and Control Department, National Authority for Remote Sensing, and Space Science, Cairo 11769, Egypt; AOCS Group, Spacecraft GNC Lab, Cairo Metropolitan Cairo 11769, Egypt; Email: tamermekky@hotmail.com

#### ARTICLE INFO

Received: 15 June 2025 | Revised: 30 July 2025 | Accepted: 10 August 2025 | Published Online: 20 August 2025 DOI: https://doi.org/10.30564/jeis.v7i2.11348

### CITATION

Habib, T.M.A., 2025. Precise Spacecraft Attitude and Angular Velocity Estimates Using Cubature Kalman Filter on Intensely Distorted One-Axis Magnetometer Measurements. Journal of Electronic & Information Systems. 7(2): 38–50. DOI: https://doi.org/10.30564/jeis.v7i2.11348

#### COPYRIGHT

Copyright © 2025 by the author(s). Published by Bilingual Publishing Group. This is an open access article under the Creative Commons Attribution-NonCommercial 4.0 International (CC BY-NC 4.0) License (https://creativecommons.org/licenses/by-nc/4.0/).

<sup>&</sup>lt;sup>1</sup> Spacecraft Dynamics and Control Department, National Authority for Remote Sensing, and Space Science, Cairo 11769, Egypt

<sup>&</sup>lt;sup>2</sup> AOCS Group, Spacecraft GNC Lab, Cairo Metropolitan Cairo 11769, Egypt

Orbit Control System (AOCS) to choose an appropriate algorithm according to mission specific key performance indices. A case study spacecraft is utilized which is subject to aerodynamics drag torques, solar radiation pressure torques, and residual magnetic torques.

Keywords: Magnetometer; Measurements; Cubature Kalman Filter; Malfunctioning; Precise

# 1. Introduction

Determining a spacecraft's attitude fundamentally relies on measuring distinct physical quantities along its body axes, including the magnetic field of the earth, the solar vector, and the horizon of the earth, etc. Magnetometers stand as the predominant sensors for this purpose. Almost every Attitude and Orbit Control System (AOCS) employs a magnetometer as its basic instrument to measure the three spatial components of the earth's magnetic field. Since magnetometers lack moving components, they typically exhibit extended durability and enhanced reliability compared to alternative sensors. Moreover, magnetometers are relatively inexpensive, thereby contributing to their widespread adoption within AOCS frameworks. These advantages serve as primary justifications for preferring and routinely selecting magnetometers as sensors in AOCS systems.

Magnetometers may be integrated with additional spacecraft orientation sensors, as demonstrated in singleframe attitude determination techniques [1]. Nonetheless, this strategy introduces specific difficulties. For instance, throughout the eclipse phase in every earth orbit, the sun sensor information becomes entirely inaccessible due to shadow effect caused by the earth. Gyroscopes similarly cannot function for extended periods as a result of error buildup. Star sensors, although usually providing high-accuracy attitude data, demand significant electrical power. In addition, they have stringent operation conditions regarding the spacecraft angular velocities which must be very low to enable the star sensor functioning. Considering common electric power limitations, star sensors might prove entirely unsuitable for lengthy operational periods. Under these circumstances, the magnetometer frequently remains the sole accessible sensor. These prolonged operational intervals commonly take place during the spacecraft's standby phase, constituting most of its service life. While in standby mode, the spacecraft must roughly sustain its orientation so that it can promptly transition to high-accuracy mode of operation at any given time indeed. Magnetometers are ideal sensors for this function. In addition to their recognized advantages, magnetometers consistently deliver the following advantages:

- 1- Prolonged operational periods;
- 2- Unremitting measurements;
- 3- Low energy usage.

On the other hand, magnetometers could not be used solely by single-frame attitude determination techniques. Furthermore, magnetometers are utilized to measure the earth's magnetic field. The magnitude of the earth's magnetic field is inversely proportional to the cubic distance measured from the earth's center. Thus, magnetometers are not suitable for usage at very high spacecraft altitudes due to the weak and even vanishing magnitudes of the earth's magnetic field. Taking into account these advantages, many research papers and scholarly theses have focused exclusively on determining spacecraft orientation purely through the use of magnetometer data alone for spacecraft orbiting the earth in Low Earth Orbits (LEO). Unfortunately, the suggested solutions face multiple serious challenges. This outcome stems from various factors. The primary reasoning is that the problem of spacecraft attitude determination (&/estimation) becomes fully observable when the vehicle is equipped with two or more sensor types. Thus, using merely one sensor type—such as a magnetometer—is typically considered extremely difficult because the system loses its full observability characteristics. System observability deteriorates significantly further when one of the three magnetometer channels unexpectedly starts malfunctioning severely. Additionally, observability declines to its lowest level when two out of three of the magnetometer channels fail. The next major source of these issues originates from the particular process of choosing appropriate representation of system states. The majority of attitude state representations documented in current literature frequently encounter singularities at particular spacecraft orientation angles. This constraint limits the wideranging application of many developed algorithms at any

given spacecraft orientation and could result in a total algorithm failure. The third issue stems from the presumption of small angles approximation. This assumption severely limits any algorithm's capacity to operate effectively only at small Euler angles. Therefore, the estimator may diverge if the initial estimation error is substantially large.

To explain these challenges, Deutschmann, and Bar-Itzhack<sup>[2]</sup> presented a Three-Axis Magnetometer (TAM) that is used to determine both the spacecraft's attitude, and orbit. However, the newly devised algorithms were capable of handling small initial orientation estimation errors confined to only 16 degrees. Psiaki et al. [3] derived the spacecraft's orientation angles solely from magnetometer measurements. Even though the developed algorithms could rectify initial attitude estimation errors up to 45 degrees, they nevertheless displayed notable limitations in this regard. Habib [4] described exhaustively numerous detailed spacecraft attitude estimation models. Markley and Mortari<sup>[5]</sup> stated that various advanced attitude determination methods are seldom used mainly because of their indeed extremely high computational demands. Such demands often restrict or even prevent the deployment of these algorithms under real-time operational conditions on the spacecraft. Remarkably, numerous commercially operating spacecraft continue to run on processors that are usually twenty years back [6]. This happens because the stringent procedure of certifying a certain processor for space applications is remarkably time-consuming. In addition, it requires successive long-duration missions with the processor in place. Algorithms similar to those proposed by Hajiyev and Cilden-Guler<sup>[7]</sup> could not be deployed on a twenty years old processor. Hajiyev and Cilden-Guler<sup>[8]</sup> investigated various methods for estimating the orientation of gyro-less satellite employing magnetometers, and sun sensors. Bak<sup>[9]</sup> presented algorithms for estimating spacecraft orientation based on magnetometer, in addition to sun sensor measurements. Nonetheless, the maximum initial attitude estimation error these algorithms can accommodate is only 60 degrees. Carletta et al. [10] utilized a TAM to estimate spacecraft attitude, although the filter demonstrated a steady-state value of the error is approximately equal to 14 degrees about the yaw direction, which is considered excessive. Hart<sup>[11]</sup> employed a magnetometer to estimate the attitude angle about the yaw motion direction, making the derivation of three-axis orientation estimates impractical. Han et al. [12]

developed an algorithm to linearly estimate spacecraft attitude using magnetometer measurements, showing a value of 3 degrees for the steady-state error, which is considered a high value. Ma<sup>[13]</sup> utilized the Unscented Kalman Filter (UKF) to estimate the attitude based on magnetometer measurements. The steady state values of the estimation errors were about 0.3 Degrees. The UKF introduced by Driedger et al. <sup>[14]</sup> faced singularity problems arising from the selection of state variables representing spacecraft orientation.

Fundamentally, the current study's aim and contribution is to present a method for estimating spacecraft orientation that relies exclusively on magnetometer measurements. This novel approach effectively tackles all the challenges previously discussed in the thorough literature review, simultaneously and efficiently, quite well. The approach introduced in this study utilizes the CKF, which was engineered to overcome linearization problems usually associated with conventional EKF algorithms. The proposed approach is compared against previously intensely verified EKF-based algorithms which were validated to estimate EGYPTSAT-1 spacecraft attitude, thereby confirming the approach's effectiveness.

The current manuscript is organized as follows: In section (2), nonlinear models of spacecraft motion are presented. In section (3), the necessary estimation algorithm for CKF is introduced. Simulation results and discussions are provided in section (4). Finally, in section (5), conclusions are summarized and future work is outlined.

# 2. Nonlinear Spacecraft Motion Models

To proceed, it is essential to present precise definitions for the coordinate systems currently in use. The Earth-Centered Inertial (ECI) coordinate system incorporates an X-axis that aims directly at the Vernal Equinox, a Z-axis pointing at the same direction of Earth's rotation, and a Y-axis which completely adheres to the right-hand system of axes. Additionally, a reference coordinate system is specified. In the reference coordinate system, the X-axis aligns with the vector of spacecraft's velocity relative to Earth, the Z-axis points directly toward Nadir, and finally the Y-axis consistently complies with the right-hand system of axes. If the spacecraft attitude angles become zero, the reference

coordinate system coincide with the another system of axes which is called spacecraft body coordinate system.

Cowell's method is notably effective in fully detailing the spacecraft's translational motion model<sup>[15]</sup>. The method is concisely presented as follows<sup>[4]</sup>:

$$\ddot{R} = -\frac{\mu_E}{\left|\left|R\right|\right|^3}R + a_a \tag{1}$$

Within ECI coordinate system, R denote position vector of the spacecraft, while  $\ddot{(})$  signifies the second derivative w.r.t. time. The gravitational constant of the earth is denoted by  $\mu_E$ , and  $a_a$  represents the perturbation acceleration resulting directly from the non-spherical shape of the earth  $^{[16]}$ . The relationship governing a spacecraft's rotational motion is fully detailed solely by the specific kinematic and dynamic equations  $^{[17,\ 18]}$ . The kinematic equations can be expressed in matrix form as

$$\dot{Q}^{I \to B} = \frac{1}{2} \overline{\omega} Q^{I \to B} \tag{2}$$

where the over dot on the symbol denotes the first derivative w.r.t. time and the transformation of a vector from ECI to the body coordinate system is performed using the quaternion vector, labeled as  $Q^{I \to B} = [q_1 \quad q_2 \quad q_3 \quad q_4]^T$ , which comprises a real segment,  $q_4$ , and complex components,  $q_1$ ,  $q_2$ , and  $q_3$ . The formula defining the matrix, labeled as  $\overline{\omega}$ , can be expressed as follows

$$\overline{\omega} = \begin{bmatrix} 0 & \omega_z & -\omega_y & \omega_x \\ -\omega_z & 0 & \omega_x & \omega_y \\ \omega_y & -\omega_x & 0 & \omega_z \\ -\omega_x & -\omega_y & -\omega_z & 0 \end{bmatrix}$$
(3)

In this context,  $\omega = \begin{bmatrix} \omega_x & \omega_y & \omega_z \end{bmatrix}^T$  represents the spacecraft's inertial angular velocities. The following relation establishes the spacecraft rotational dynamics [17],

$$\dot{\omega} = I^{-1}[(I\omega + H_{\omega})\times]\omega + I^{-1}(M_a + M_a + M_r + M_s) + w_k$$

$$(4)$$

where  $M_g$ ,  $M_a$ ,  $M_m$ , and  $M_s$ , indicate torques produced by gravity gradient, aerodynamic forces, residual magnetic influences, solar radiation pressure respectively. Details of computing such disturbance torques are lengthy, and presented by Habib<sup>[4]</sup>.  $H_\omega$  signifies the angular momentum vector of any moving components inside the spacecraft,  $w_k$  represents a zero-mean white Gaussian noise associated with the process noise. Detailed procedures for calculating disturbance torques are provided by Habib<sup>[16]</sup>.  $[\beta \times]$  constitutes the cross product equivalent matrix for the vector,

$$\beta = \begin{bmatrix} \beta_x & \beta_y & \beta_z \end{bmatrix}^T$$
, defined as

$$[\beta \times] = \begin{bmatrix} 0 & -\beta_z & \beta_y \\ \beta_z & 0 & -\beta_x \\ -\beta_y & \beta_x & 0 \end{bmatrix}$$
 (5)

and the spacecraft's moment of inertia matrix, I, is expressed as

$$I = \begin{bmatrix} I_{xx} & -I_{xy} & -I_{xz} \\ -I_{xy} & I_{yy} & -I_{yz} \\ -I_{xz} & -I_{yz} & I_{zz} \end{bmatrix}$$
(6)

Choosing the state vector that represents a spacecraft's orientation dynamics is essential, acting as a key component for every attitude estimation algorithm. Consequently, the state vector is selected as

$$X = \begin{bmatrix} q_1 & q_2 & q_3 & q_4 & \omega_x & \omega_y & \omega_z \end{bmatrix}$$
 (7)

The state vector chosen in Equation (7) presents the extremely valuable feature of accurately representing every attitude maneuver entirely without encountering any singularity, thus successfully preventing the blow-up of the overall algorithm because of singularities. Additionally, it permits the precise portrayal of maneuvers encountering large attitude angles. Furthermore, selecting the state vector if the orbital motion as clearly depicted in Equation (1) guarantees singularity free performance specific orbit types.

The state vector is projected ahead of time through the relation.

$$\hat{X}_{k}^{(-)} = f(\hat{X}_{k-1}) \tag{8}$$

where f represents a nonlinear function that characterizes system behavior. In this instance, f, is explicitly derived by merging Equations (2) and (4). Thus,

$$f(X) = \frac{\frac{1}{2}\omega Q^{I \to B}}{\left[I^{-1}\left[(I\omega + H_{\omega}) \times \right]\omega + I^{-1}\left(M_g + M_a + M_r + M_s\right)\right]}$$
(9)

Thus, the measurement vector,  $z_k$ , is defined by

$$z_k(X_k) = B_B = D^{I \to B}(Q^{I \to B})B_I + v_k$$
 (10)

where,  $B_B$ , denotes the Earth's magnetic field vector observed in spacecraft body coordinate system,  $B_I$ , denotes Earth's magnetic field vector represented in the ECI, and  $D^{I \to B}$  denotes the transformation matrix from ECI to body coordinate system. The transformation matrix,  $D^{I \to B}$ , can be expressed as [17].

$$D^{I \to B} \left( Q^{I \to B} \right) = \begin{bmatrix} q_1^2 - q_2^2 - q_3^2 + q_4^2 & 2(q_1 q_2 + q_3 q_4) & 2(q_1 q_3 - q_2 q_4) \\ 2(q_1 q_2 - q_3 q_4) & -q_1^2 + q_2^2 - q_3^2 + q_4^2 & 2(q_2 q_3 + q_1 q_4) \\ 2(q_1 q_3 + q_2 q_4) & 2(q_2 q_3 - q_1 q_4) & -q_1^2 - q_2^2 + q_3^2 + q_4^2 \end{bmatrix}$$
(11)

# 3. Spacecraft Attitude Estimation Al- 1, 2, ..., 2N), through system dynamics to relieve the problems encountered while computing the partial derivatives of

The primary responsibility of any algorithm crafted to ascertain spacecraft attitude is to determine the vehicle's attitude with utmost precision, employing a collection of measurements that might contain inaccuracies. Algorithms that rely on Singular Value Decomposition (SVD) are generally disfavored owing to their considerable computational cost<sup>[5]</sup>. This results from the extremely limited processing power inherently accessible on board a spacecraft throughout its orbit. Consequently, algorithms based on the Extended Kalman Filter (EKF) have been widely adopted due to their exceptional versatility in various applications. Utilizing these EKF-based techniques, an effective real-time algorithm can be developed by following steps outlined below:

#### 3.1. Cubature Kalman Filter

The UKF, or alternatively Sigma Points Kalman filter, propagates a number of sigma points,  $\chi_{(i)}^{k-1}$  (i=

 $1,2,\ldots,2N$ ), through system dynamics to relieve the problems encountered while computing the partial derivatives of the nonlinear differential equations describing the process and measurement models. The Derivative Free Implementation of the EKF (DFEKF) belongs to the same family of UKF, and adopts a similar approach to it. In the DFEKF approach, only N sigma points are propagated. The Cubature Kalman Filter CKF was First developed by Arasaratnam [19, 20]. Afterwards, a very good summary for the CKF is given by Garcia et al. [21]. A primary advantage of CKF, is that it possesses no tunable parameters such as those associated with UKF, and DFEKF. Within the context summarized by Garcia et al. [21], (2N) cubature points are generated (where N is the size of the state vector) according to the relations

$$\chi_{k-1}^{(i)} = \sqrt{P_{k-1}} \xi^{(i)} + \hat{X}_{k-1} \tag{12}$$

Where

$$\xi^{(i)} = \sqrt{N} \{1\}_i \tag{13}$$

And,

$$\{1\}_{i} = \left\{ \begin{bmatrix} 1\\0\\\vdots\\0\\1\\1 \end{bmatrix}, \begin{bmatrix} 0\\1\\\vdots\\0\\2 \end{bmatrix}, \dots, \begin{bmatrix} 0\\0\\\vdots\\1\\N \end{bmatrix}, \begin{bmatrix} -1\\0\\\vdots\\0\\1\\1 \end{bmatrix}, \begin{bmatrix} 0\\-1\\\vdots\\0\\2 \end{bmatrix}, \dots, \begin{bmatrix} 0\\0\\\vdots\\-1\\N \end{bmatrix} \right\}$$

$$(14)$$

Now all of the generated (2N) points are projected a head of time through the relation

$$\chi_k^{(i)} = f(\chi_{k-1}^{(i)}), \text{ Where } J = 0, 1, 2, \dots, 2N$$
 (15)

The propagated state estimate, and covariance matrix could be calculated from

$$\hat{X}_{k}^{-} = \frac{1}{2N} \sum_{i=1}^{2N} \chi_{k}^{(i)}$$
 (16)

$$P_{k}^{-} = \frac{1}{2N} \sum_{i=1}^{2N} \left[ \chi_{k}^{(i)} \left( \chi_{k}^{(i)} \right)^{T} \right] - \left[ \hat{X}_{k}^{-} \left( \hat{X}_{k}^{-} \right)^{T} \right] + Q_{k-1}$$
(17)

Regenerate the cubature points according to the relation

$$\chi_{kR}^{(i)} = \sqrt{P_k^-} \xi^{(i)} + \hat{X}_k^- \tag{18}$$

A set of measurement could be generated at each cubature point using the relation

$$Z_{i,k} = z\left(\chi_{kR}^{(i)}\right) \tag{19}$$

$$\hat{z}_k = \frac{1}{2N} \sum_{i=1}^{2N} Z_{i,k} \tag{20}$$

Now the state of the system could be updated after

obtaining the measurements via the relations

$$P_{zz} = \frac{1}{2N} \sum_{i=1}^{2N} \left[ Z_{i,k} Z_{i,k}^T \right] - \left[ \hat{z}_k \hat{z}_k^T \right] + R_k \qquad (21)$$

$$P_{xz} = \frac{1}{2N} \sum_{i=1}^{2N} \left( \chi_k^{(i)} Z_{i,k} \right) - \left[ \hat{X}_k \hat{z}_k^T \right]$$
 (22)

$$K_k = P_{xz} \left( P_{zz} \right)^{-1}$$
 (23)

$$\hat{X}_{k}^{(+)} = \hat{X}_{k}^{(-)} + K_{k} \left[ z_{k} - \hat{z}_{k} \right]$$
 (24)

$$P_k = P_{xx} - K_k P_{zz} K_k^T \tag{25}$$

Given that the matrix representing the measurement noise covariance in its discrete form,  $R_k$ , is directly linked to its continuous version, R(t), according to the relation<sup>[22]</sup>.

$$R_k = R(t)/\Delta T \tag{26}$$

Similarly, the matrix representing process noise covariance in its discrete form,  $Q_k$ , is directly linked to its continuous form, Q, via the relation<sup>[23]</sup>.

$$Q_k = \int_{0}^{\Delta T} A(t_{k+1}, \eta) Q A(t_{k+1}, \eta)^T d\eta$$
 (27)

And,  $\eta$ , indicates time variable.

#### 3.2. Observability

Floquet theory can be applied to ensure observability of the discrete filter system by evaluating the relation<sup>[3]</sup>.

$$\Theta = \prod_{k=1}^{N} \left[ I_{3\times 3} - K_{k+1} H_{k+1} \right] \Lambda_{k+1}$$
 (28)

Where,  $I_{3\times 3}$  is a third order identity matrix  $H_{k+1}$ , is the measurement matrix, and  $\Lambda_{k+1}$ , is the state transition matrix. Every eigenvalue of the matrix,  $\Theta$ , must have a modulus less than one in the filter's steady state region to guarantee that the estimator stays stable. Additionally, the very low largest eigenvalue clearly reflects an excellent convergence speed.

# 4. Case Studies, and Discussions

The proposed CKF is compared with earlier verified EKF-based algorithms<sup>[24, 25]</sup> corresponding to the satellite EGYPTSAT-1, launched into a low-earth-orbit during April 2007. It was the first satellite of the National Authority for

Remote Sensing and Space Sciences (NARSS). The satellite emerged as Egypt's inaugural remote sensing spacecraft. Parameters for EGYPTSAT-1 were derived from different design simulations carried out during multiple spacecraft development stages, and these parameters were presented by Habib<sup>[26]</sup>. The benchmarked EKF was proposed, and verified as given by Habib [4, 26]. All of the presented estimation algorithms are initialized with zeroes. This is due to the fact that during the detumbling mode of EGYPTSAT-1 no initial attitude estimates are available to initialize the filter. Simulation time step is 4 seconds. The standard deviation of TAM error is equal to 200 nT on each sensor axis, and this is considered to be an exceptionally large value. Moreover, the maximum acceptable error in attitude angles is roughly 5 degrees in the case of low-accuracy modes of operation. For high-accuracy modes, the maximum acceptable error in attitude angles is about 0.5 degrees around each spacecraft body axis. This helps to preserve overall spacecraft stability and achieving optimal operational accuracy. The residual magnetic dipole moment is [0.3 0.3 0.3] A.m<sup>2</sup>. The spacecraft inertia matrix is given as

$$I = \begin{bmatrix} 11.2 & -0.02 & 0.08 \\ -0.02 & 11.4 & -0.2 \\ 0.08 & -0.2 & 9.2 \end{bmatrix} \text{Kg.m}^2$$
 (29)

The momentum wheel has an inertia of 1 Kg.m<sup>2</sup> with a constant angular velocity of 0.1 rad/sec in the negative Y-axis direction of the spacecraft body axes. Regarding the spacecraft orbital parameters, the spacecraft had a circular orbit with an altitude of 668 Km, an inclination angle of 98.085°. the argument of perigee angle was 69°. The true anomaly angle is zero. Finally, the Right Ascension of Ascending Node (RAAN) angle has a value of 337.5°. The spacecraft epoch time is 17 Apr, 2007 00h:00m,00s.

# Case Study 1 (Fully Functioning TAM Channels)

In Case Study 1, All of the TAM channels are functioning properly. The proposed CKF is benchmarked against EKF-based algorithms which include the EKF, DFEKF, the Sequential EKF (SEKF), UKF, and Pseudo-Linear Kalman Filter (PSELIKA). **Figure 1** vividly displays the progression over time for the estimation errors of EGYPTSAT-1 attitude. As depicted in **Figure 1**, the estimation error was initially large due to the initial absence of any spacecraft attitude information. This error starts immediately to diminish to near

zero. This indicates the success of the portrayed estimation algorithms. Figure 2 precisely depicts the estimation error of EGYPTSAT-1 angular velocities, and shows a similar performance regarding the estimation error. The success of angular velocity estimation process is a bi-product of the success of the attitude estimation process. Usually, the designer of the spacecraft attitude determination subsystem is mainly concerned with the attitude estimation error. Thus, only attitude estimation errors are portrayed in the remaining case studies. We should also note that in in Figure 1 during the steady state region of the estimators, the curves of different estimators are nearly coinciding. So, a zoom in is shown in the upper right corner of the figure. Figures 1 and 2 show that, the estimation

errors of CKF, and EKF- based algorithms align perfectly. This confirms equal accuracy performance for every filter. Moreover, these figures indicate that the CKF reaches the steady-state performance level within only half orbital period. This notable achievement is indeed extraordinary, since both the CKF and EKF- based algorithms reliably and consistently converge even when confronted with considerable initial attitude estimation errors which are—up to 85 degrees about the pitch direction and 170 degrees about the yaw direction—that are commonly observed during detumbling mode. Accordingly, the newly designed CKF algorithm is highly adaptable and could be applied during all the operational modes of a spacecraft operational.

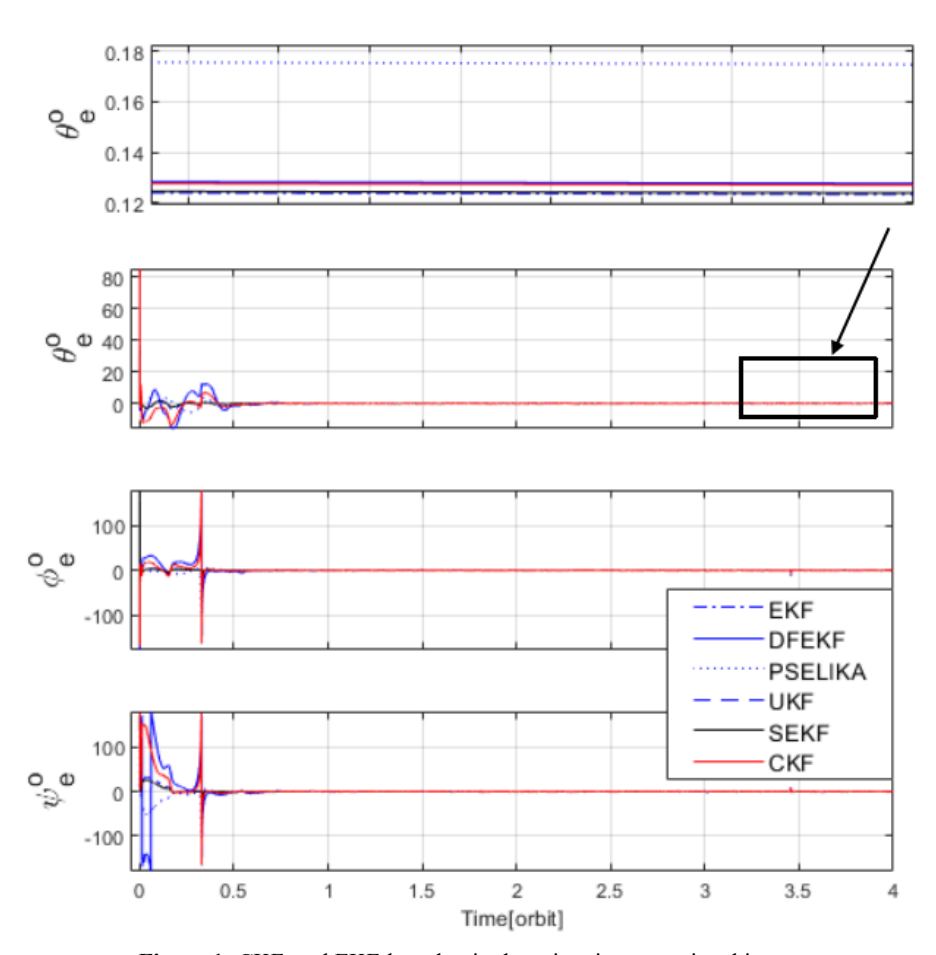


Figure 1. CKF, and EKF-based attitude estimation error time history.

CKF computations are completed on a desktop personal computer (PC) regularly having 8 GB RAM, and i7 processor operating at a speed of 3.4 GHz. **Table 1** presents accuracy, and the time required to execute the different estimation algorithms. **Table 1** clearly shows that CKF, and

EKF- based algorithms demonstrate very low estimation error values compared with the maximum allowed value of the angular error. We should take into consideration that measurement error of the TAM is significantly higher than the values reported in other investigations (which frequently

used a TAM error standard deviation having a value of 50 nT or up to 100 nT) under similar rigorous testing conditions. Thus, the developed estimation algorithm is capable of utilizing lower cost TAMs characterized by low accuracy to achieve low attitude estimation errors. Given the achieved accuracy, TAM is capable to serve as a single attitude sensor during any operational mode.

As shown in Table 1, CKF and the EKF- based algorithms reach remarkably comparable accuracy levels. The average, maximum, and minimum execution time presented in Table 1 shows nearly identical figures among CKF, DFEKF, and UKF. This stems from the fact that all of these algorithms alleviate totally the problems encountered due to overall system nonlinearity through propagation of number of sigma or cubature points. We should note that simulations are done on a desktop personal computer (PC). Thus, algorithm execution time may vary due to other tasks related to operating system tasks scheduled to run on the processor. More accurate results could be obtained when applying the algorithm on a real flight processor as suggested in the future work section. In addition, as observed in Table 1 the DFEKF has a lower average execution time compared to CKF, and UKF. This is due to the fact that DFEKF depends on propagating N Sigma points, and both CKF, and UKF propagates 2N sigma points. Also, CKF has a lower average execution time compared to CKF due to the difference among the governing equations of both filters.

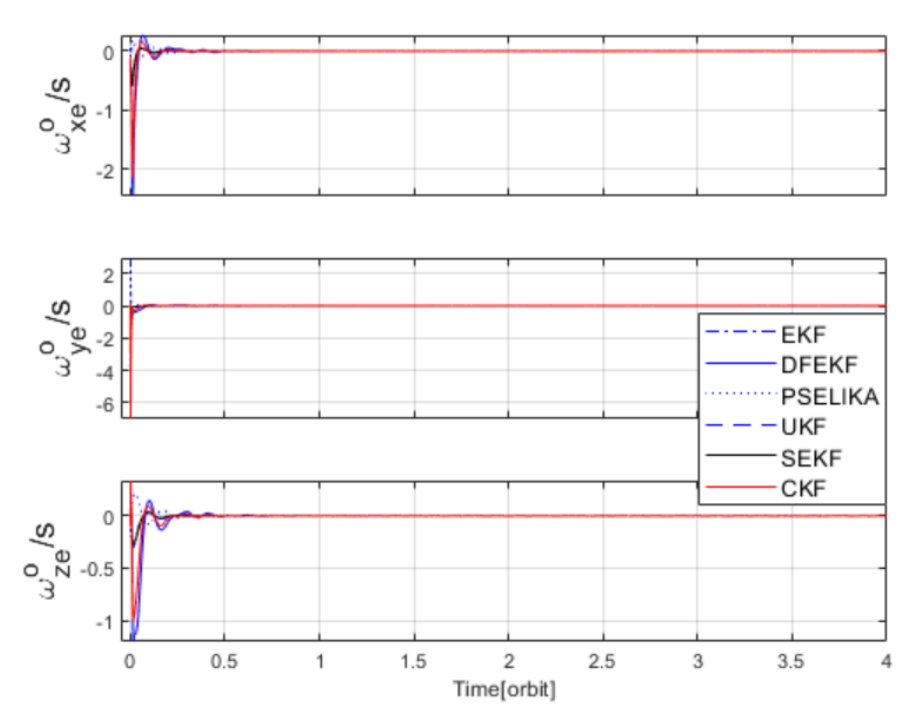


Figure 2. CKF, and EKF-based angular velocity estimation error time history.

Table 1. Performance criteria of CKF, and EKF- based algorithms (Case Study 1).

	Pitch Angle Error Standard Deviation (deg.)	Yaw Angle Error Standard Deviation (deg.)	Roll Angle Error Standard Deviation (deg.)	Maximum Execution Time (s)	Average Execution Time (s)	Minimum Execution Time (s)
DFEKF	0.06	0.24	0.24	0.14	0.07	0.07
PSELIKA	0.07	0.32	0.31	0.11	0.07	0.07
EKF	0.05	0.25	0.24	0.41	0.07	0.07
SEKF	0.06	0.25	0.24	0.12	0.07	0.07
UKF	0.06	0.24	0.24	0.2	0.1	0.08
CKF	0.06	0.24	0.24	0.1	0.08	0.08

EKF. Both filters were run on a PC, where the  $\alpha\beta$  filter s execution time. The CKF developed herein obtained a

Boussadia et al. [27] developed  $\alpha\beta$  filter compared to obtained 0.39 s execution time of, the EKF reported 0.74

maximum measured execution time of 0.108 s. This plainly demonstrates the improved efficiency of the created CKF algorithm. Furthermore, it should be emphasized that this current study avoids utilizing any simplifying assumption associated with small angles. This enabled the CKF to efficiently handle significant initial estimation errors and reliably reach remarkably highly accurate outcomes.

Based on the abovementioned results, the developed CKF have the following benefits relative to the referenced studies:

- Convergence even with considerable initial estimation error.
- 2- Diminished error values of attitude estimates (yielding a 0.24 degrees standard deviation) when compared with the preset maximum error threshold, specifically set at approximately  $\pm 0.5$  degrees.

# Case Study 2 (x, and y TAM Channels only are functioning)

In the second case, spacecraft parameters are exactly the same as those used in the first case. We assume the TAM has a malfunctioning z-channel. Thus, the measurements of x, and y channels are the only existing measurements.

Figure 3 portrays the performance of different estimation algorithms in terms of the errors of the attitude estimation process. As depicted in Figure 3, estimation errors from CKF and EKF-based algorithms coincide entirely. This indicates that both filters achieve the same accuracy. Furthermore, all of the filters reach steady-state region of their performance just after a period of 1.5 orbits, a duration that is somewhat longer than Case 1. This happens because only two unique measurements are accessible at any given time rather than three. Consequently, all of the estimation algorithms demand extra time and further measurements to eventually converge successfully. As clearly illustrated in this figure, just after the period of 1.5 orbits, the attitude estimation errors are almost identical for every single attitude estimation method. Figure 4, displays the maximum Eigenvalue time history for the CKF. As shown in this figure, the maximum Eigenvalue has values much below 1, thus indicating good observability.

**Table 2** shows different performance indicators for different estimation algorithms in the case of faulty z-channel. In Case Study 2, the steady-state error values of the estimators are slightly higher than those normally observed in Case Study 1. This increase is due to having only two measurements available at any moment instead of three.

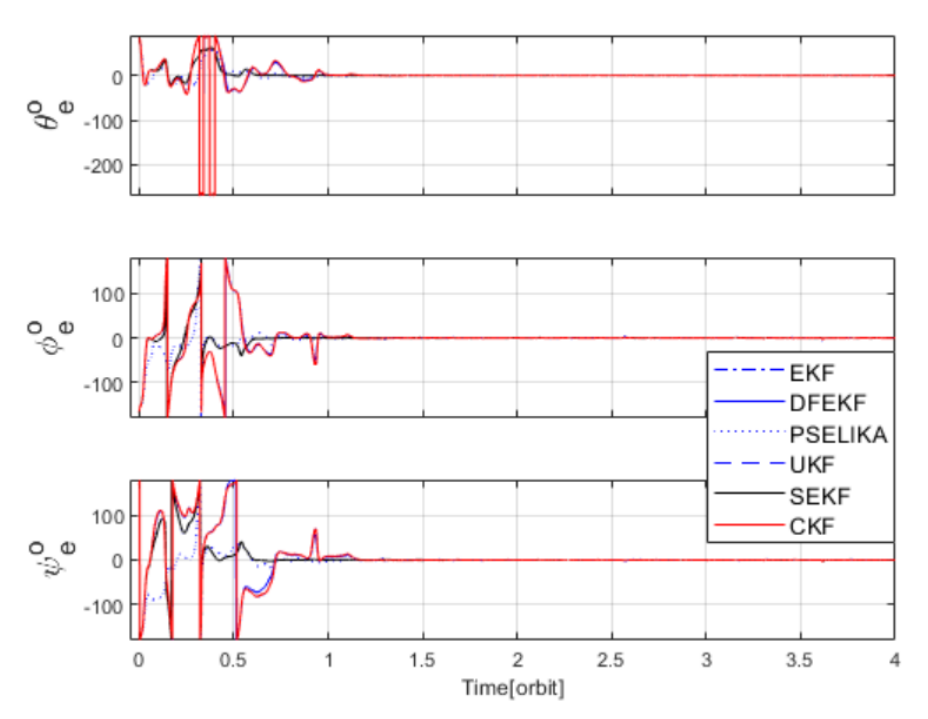


Figure 3. CKF, and EKF-based attitude estimation error time history (Case Study 2).

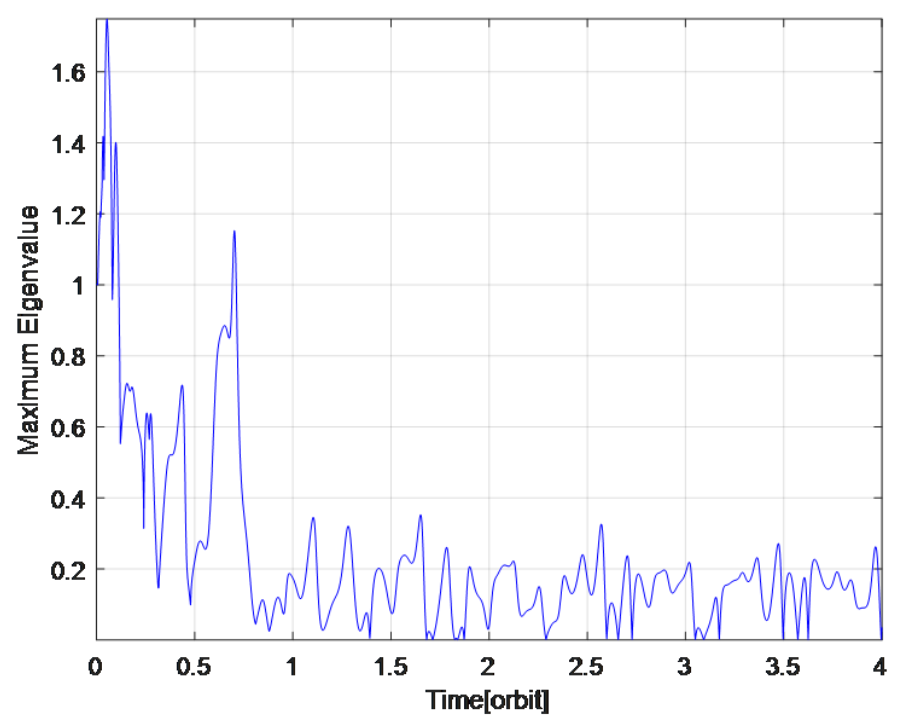


Figure 4. CKF maximum Eigenvalue time history (Case Study 2).

18	abie 2.	Periorn	nance	e criteria	OI CKF	, and	EKF-0	asea a	igorithr	ns (Case	Study	2).

	Pitch Angle Error Standard Deviation (deg.)	Yaw Angle Error Standard Deviation (deg.)	Roll Angle Error Standard Deviation (deg.)	Maximum Execution Time (s)	Average Execution Time (s)	Minimum Execution Time (s)
DFEKF	0.06	0.21	0.21	0.16	0.07	0.07
PSELIKA	0.09	0.39	0.38	0.12	0.07	0.07
EKF	0.06	0.22	0.22	0.97	0.07	0.07
SEKF	0.06	0.22	0.22	0.11	0.07	0.07
UKF	0.06	0.21	0.21	0.22	0.08	0.08
CKF	0.06	0.21	0.21	0.18	0.08	0.08

#### Case Study 3 (x TAM Channel only is functioning)

In Case 3, the same spacecraft parameters of Case Study 1 were utilized. In Case Study 3, it is assumed the only available measurements are coming from the TAM x-channel. **Figure 5** displays the complete record of attitude estimation errors based on measurements from the x-channel only. As shown in **Figure 5**, CKF, and EKF- based algorithms estimation errors, are exactly identical. This assures CKF high accuracy. All of the estimation algorithms reach steady state solutions after six orbits, which is a longer period compared to Cases 1 and 2. This delay results from having only a single measurement channel accessible at any time, instead of two or three measurement channels provided previously.

Therefore, all of the estimators need excess number of measurements from the x-channel compared to Case study 1, and Case Study 2, to converge successfully.

Table 3 clearly shows the key performance indicators for different estimation algorithms in Case Study 3. In Case study 3, the estimators' steady-state errors were higher than those obtained in cases 1, and 3. Again this is because of that the only available measurements are those corresponding to a single channel instead of two or three as in cases 1, and 2. It is crucial to mention that the values of the steady-state errors consistently remain well below the predetermined threshold of 0.5 degrees requirement of the high-accuracy mode of operation. Therefore, CKF could effectively operate when a single magnetometer channel measurements are available.

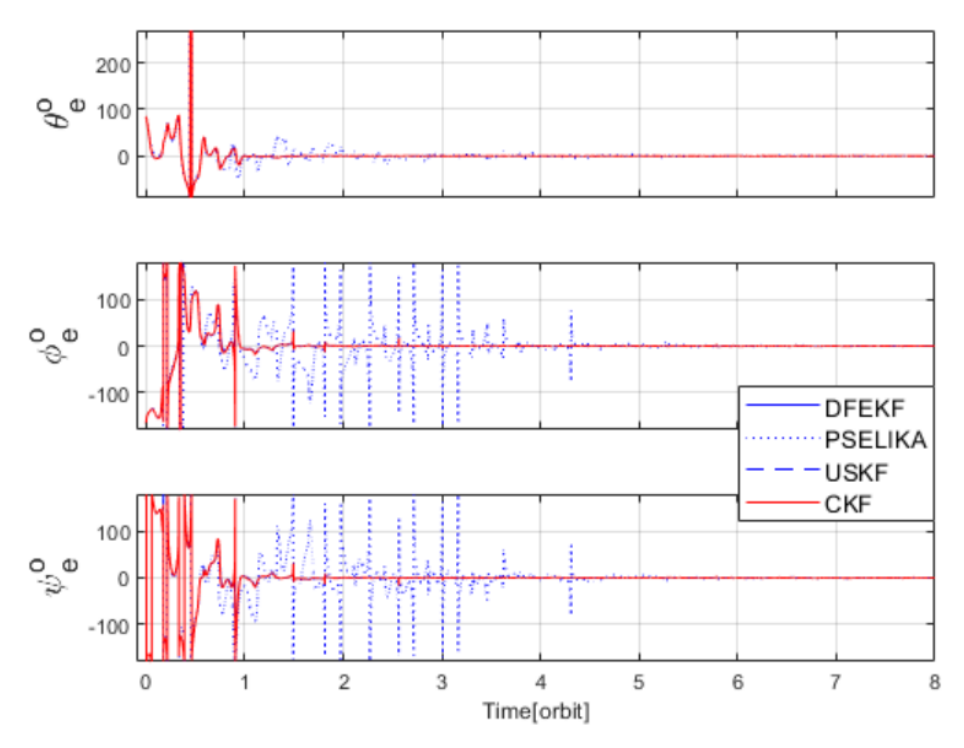


Figure 5. CKF, and EKF-based attitude estimation error time history (Case Study 3).

Table 3. Performance criteria of CKF, and EKF- based algorithms (Case Syudy 3).

	Pitch Angle Error Standard Deviation (deg.)	Yaw Angle Error Standard Deviation (deg.)	Roll Angle Error Standard Deviation (deg.)	Maximum Execution Time (s)	Average Execution Time (s)	Minimum Execution Time (s)
PSELIKA	0.17	0.41	0.42	0.14	0.07	0.07
DFEKF	0.09	0.20	0.09	0.15	0.07	0.07
UKF	0.09	0.20	0.19	0.2	0.08	0.08
CKF	0.09	0.20	0.19	0.18	0.08	0.08

## 4.1. Conclusions

In this paper, we develop a precise technique for determining spacecraft orientation angles and angular velocities using only a TAM. The innovative approach utilized a CKF formulation and was rigorously compared against previously intensely verified EKF-based algorithms. The CKF method achieved the same accuracy as DFEKF, and UKF. It achieved attitude precision of no less than 0.24 degrees per axis, permitting use without extra sensors. The procedure bypassed any approximation pertaining to small angles by modeling spacecraft attitude using quaternions, thus sidestepping the singularity problems linked to large spacecraft attitude angles. The CKF approach clearly demonstrated convergence ability even when initial attitude estimation errors were as high as 170 degrees.

Moreover, the developed method consistently produced highly accurate estimates of spacecraft attitude even when the magnetometer's z-channel malfunctioned. When the y-channel and z-channel failed, the proposed CKF still managed to provide fully satisfactory attitude estimates appropriate for high-precision operational modes.

Future research efforts are planned to deploy the developed CKF algorithm within a Hardware-In-The-Loop Simulator (HIL) testing setup soon. NARSS intends to construct an earth observing spacecraft mission. Thus, the name of the spacecraft is suggested to be NARSS Earth Observation Satellite (NEOSat-1). Thus, a HIL is to be constructed for NEOSat-1. Challenges such as limited computational resources, and real time optimization could be solved via a dedicated software team which could apply the developed algorithm herein to specific hardware configuration. Rapid

development of high speed processors could also serve software developers to solve the aforementioned challenges. The accuracy of computing algorithm execution time may be enhanced through applying the developed algorithm to the real flight processor. Accordingly, it is planned to utilize the developed CKF algorithms on a real spacecraft mission, initially as reserve solutions aboard NEOSat-1. In a subsequent phase, the proposed CKF algorithm is expected to function as the primary provider of attitude estimates effectively. Moreover, the dependent state quantity,  $q_4$ , could be completely omitted from the spacecraft representing state vector, X, in future work, and the resulting algorithm performance is to be evaluated. Besides, the developed algorithm herein is planned to be modified to deal with non-Gaussian white noise, and compared against other forms of Particle Filter (PF). Also, a separate complete parametric study could be established over different spacecraft orbits, different spacecraft attitude parameters, in addition to different TAM characteristics.

# **Funding**

The author affirms that this study is financed by NARSS under project code 0785/SR/SPA/2025. Open access funding support is provided by Journal of Electronic & Information Systems.

# **Institutional Review Board Statement**

Not applicable.

# **Informed Consent Statement**

Not applicable.

# **Data Availability Statement**

Data generated during the current study are shown graphically on manuscript figures.

# **Conflict of Interest**

The author asserts that there are no further financial interests connected with the study detailed in this manuscript.

# References

- [1] Guler, D., Conguroglu, E., Hajiyev, C., 2017. Single-Frame Attitude Determination Methods for Nano-Satellites. Metrology and Measurement Systems. 24(2), 313–324. DOI: https://doi.org/10.1515/mms-2017-0023
- [2] Deutschmann, J., Bar-Itzhack, I.Y., 2001. Evaluation of Attitude and Orbit Estimation Using Actual Earth Magnetic Field Data. Journal of Guidance Control and Dynamics. 24(3), 616–623. DOI: https://doi.org/10. 2514/2.4753
- [3] Psiaki, M., Martel, F., Pal, P., 1990. Three-Axis Attitude Determination via Kalman Filtering of Magnetometer Data. Journal of Guidance Control and Dynamics. 13(3), 506–514. DOI: https://doi.org/10.2514/3.25364
- [4] Habib, T., 2009. New Algorithms of Nonlinear Spacecraft Attitude Control via Attitude, Angular Velocity, and Orbit Estimation Based on the Earth's Magnetic Field [PhD Thesis]. Cairo University: Cairo, Egypt.
- [5] Markley, F.L., Mortari, D., 2000. Quaternion Attitude Estimation Using Vector Observations. Journal of the Astronautical Sciences. 48(2), 359–380. DOI: https://doi.org/10.1007/BF03546284
- [6] Habib, T., 2022. Spacecraft Attitude and Orbit Determination from the Cost and Reliability Viewpoint: A Review. ASRIC Journal on Natural Sciences. 1, 14–35.
- [7] Hajiyev, C., Cilden-Guler, D., 2022. Attitude and Gyro Bias Estimation by SVD-Aided EKF. Measurement. 205, 112209. DOI: https://doi.org/10.1016/j.measur ement.2022.112209
- [8] Hajiyev, C., Cilden-Guler, D., 2016. Review on Gyroless Attitude Determination Methods for Small Satellites. Progress in Aerospace Sciences. 90, 54–66. DOI: https://doi.org/10.1016/j.paerosci.2017.03.003
- [9] Bak, T., 1999. Spacecraft Attitude Determination a Magnetometer Approach [PhD Thesis]. Aalborg University, Department of Control Engineering: Aalborg, Denmark.
- [10] Carletta, S., Teofilatto, P., Farissi, M., 2020. A Magnetometer-Only Attitude Determination Strategy for Small Satellites: Design of the Algorithm and Hardware-in-the-Loop Testing. Aerospace. 7(1), 1–21. DOI: https://doi.org/10.3390/aerospace7010003
- [11] Hart, C., 2009. Satellite Attitude Determination Using Magnetometer Data Only. In Proceedings of the 47th AIAA Aerospace Sciences Meeting Including The New Horizons Forum and Aerospace Exposition, Orlando, FL, USA, 5–8 January 2009; pp. 1–11. DOI: https://doi.org/10.2514/6.2009-220
- [12] Han, K., Wang, H., Jin, Z., 2010. Magnetometer-Only Linear Attitude Estimation for Bias Momentum Pico-Satellite. Journal of Zhejiang University Science A (Applied Physics & Engineering). 11(6), 455–464. DOI:

- https://doi.org/10.1631/jzus.A0900725
- [13] Ma, G., 2005. Unscented Kalman Filter for Spacecraft Attitude Estimation and Calibration Using Magnetometer Measurements. In Proceedings of the Fourth International Conference on Machine Learning and Cybernetics, Guangzhou, China, 18–21 August 2005; pp. 18–21. DOI: https://doi.org/10.1109/ICMLC.2005.1526998
- [14] Driedger, M., Rososhansky, M., Ferguson, P., 2020. Unscented Kalman Filter-Based Method for Spacecraft Navigation Using Resident Space Objects. Aerospace Systems. 3, 197–205. DOI: https://doi.org/10.1007/ s42401-020-00055-w
- [15] Srivastava, V., Mishra, P., Ramakrishna, B., 2021. Satellite Ephemeris Prediction for the Earth Orbiting Satellites. Aerospace Systems. 4, 323–334. DOI: https://doi.org/10.1007/s42401-021-00092-z
- [16] Habib, T., 2022. Artificial Intelligence for Spacecraft Guidance, Navigation, and Control: A State-of-the-Art. Aerospace Systems. 5, 503–521. DOI: https://doi.org/10.1007/s42401-022-00152-y
- [17] Sidi, M.J., 1997. Spacecraft Dynamics and Control, a Practical Engineering Approach. Cambridge University Press: Cambridge, UK. DOI: https://doi.org/10. 1017/CBO9780511815652
- [18] Fu, J., Chen, L., Zhang, D., et al., 2022. Orbit–Attitude Dynamics and Control of Spacecraft Hovering Over a Captured Asteroid in the Earth–Moon System. Aerospace Systems. 5, 265–275. DOI: https://doi.org/10.1007/s42401-021-00122-w
- [19] Arasaratnam, I., 2009. Cubature Kalman Filtering: Theory & Applications [PhD Thesis]. McMaster University: Hamilton, ON, Canada.
- [20] Arasaratnam, I., Haykin, S., 2009. Cubature Kalman Filters. IEEE Transactions on Automatic Control. 54(6), 1254–1269.

- [21] Garcia, R., Pardal, P., Kuga, H., et al., 2019. Nonlinear Filtering for Sequential Spacecraft Attitude Estimation with Real Data: Cubature Kalman Filter, Unscented Kalman Filter and Extended Kalman Filter. Advances in Space Research. 63, 1038–1050.
- [22] Brown, R.G., Hwang, P.Y., 1997. Introduction to Random Signals and Applied Kalman Filtering. John Wiley and Sons, Inc.: Hoboken, NJ, USA. pp. 290–291.
- [23] Smyth, A., Wu, M., 2007. Multi-Rate Kalman Filtering for the Data Fusion of Displacement and Acceleration Response Measurements in Dynamic System Monitoring. Mechanical Systems and Signal Processing. 21, 706–723. DOI: https://doi.org/10.1016/j.ymssp.2006. 03.005
- [24] Habib, T., 2023. Three-Axis High-Accuracy Spacecraft Attitude Estimation via Sequential Extended Kalman Filtering of Single-Axis Magnetometer Measurements. Aerospace Systems. 6, 356–374. DOI: https://doi.org/ 10.1007/s42401-023-00221-w
- [25] Habib, T., 2023. Magnetometer-Only Kalman Filter Based Algorithms for High Accuracy Spacecraft Attitude Estimation (A Comparative Analysis). International Journal of Robotics and Control Systems. 3(3), 433–448.
- [26] Habib, T., 2013. A Comparative Study of Spacecraft Attitude Determination and Estimation Algorithms (A Cost-Benefit Approach). Aerospace Science and Technology. 26(1), 211–215. DOI: https://doi.org/10.1016/ j.ast.2012.04.005
- [27] Boussadia, H., Mohammed, M.A.S., Boughanmi, N., et al., 2022. A Combined Configuration (αβ Filter TRIAD Algorithm) for Spacecraft Attitude Estimation Based on In-Orbit Flight Data. Aerospace Systems. 5, 223–232. DOI: https://doi.org/10.1007/s42401-021-00115-9